



A study of the $\gamma^*-f_0(980)$ transition form factors

P. Kroll^{1,2,a}

¹ Fachbereich Physik, Universität Wuppertal, 42097 Wuppertal, Germany

² Institut für Theoretische Physik, Universität Regensburg, 93040 Regensburg, Germany

Received: 12 October 2016 / Accepted: 30 January 2017 / Published online: 13 February 2017

© The Author(s) 2017. This article is published with open access at Springerlink.com

Abstract The $\gamma^*-f_0(980)$ transition form factors are calculated within the QCD factorization framework. The f_0 -meson is assumed to be mainly generated through its $s\bar{s}$ Fock component. The corresponding spin wave function of the $f_0(980)$ meson is constructed and, combined with a model light-cone wave function for this Fock component, used in the calculation of the form factors. In the real-photon limit the results for the transverse form factor are compared to the large momentum-transfer data measured by the BELLE collaboration recently. It turns out that, for the momentum-transfer range explored by BELLE, the collinear approximation does not suffice, power corrections to it, modeled as quark transverse moment effects, seem to be needed. Mixing of the f_0 with the $\sigma(500)$ is also briefly discussed.

1 Introduction

Recently the BELLE collaboration [1] has measured the cross section for $\gamma^*\gamma \rightarrow \pi^0\pi^0$ for large photon virtuality, Q_1^2 , and small energy in the $\gamma^*\gamma$ center-of-mass system. From these data the photon-meson transition form factors have been extracted for the scalar, $f_0(980)$, and tensor, $f_2(1270)$, mesons for $Q_1^2 \lesssim 30 \text{ GeV}^2$. These transition form factors are similar to those for the pseudoscalar mesons which have been extensively studied by both experimentalists and theoreticians. In Ref. [2] the $\gamma - f_0$ and the $\gamma - f_2$ form factors have been investigated within the NRQCD factorization framework [3,4], in which relativistic corrections and higher Fock state contributions are suppressed by powers of the relativistic velocity of the quarks in the meson, i.e. up to some minor modifications, the light mesons are treated like heavy Quarkonia. Super-convergence relations have been derived in [5] and shown to provide constraints on the $\gamma - f_2$ transition form factor. The latter form factor has also been studied within the framework of collinear factorization [6]. A

phenomenological model for this form factor is discussed in [7,8]. The process $\gamma^*\gamma \rightarrow \pi\pi$ has been discussed in the framework of generalized distribution amplitudes, time-like versions of generalized parton distributions [9]. In this paper the interest is focused on the $\gamma - f_0$ transition form factor.

The $f_0(980)$ meson is a complicated system whose nature is not yet fully understood. Its peculiar properties have led to many speculations about its quark content. A comparison of the partial widths for the f_0 decays into pairs of pions and Kaons [10] under regard of the respective phase spaces reveals that the matrix element for $f_0 \rightarrow K^+K^-$ is much larger than that for $f_0 \rightarrow \pi^+\pi^-$. Thus, if the f_0 is viewed as a quark-antiquark state, it is dominantly an $s\bar{s}$ state. The comparison of the branching ratios for the radiative decays of the ϕ -meson into the f_0 and π^0 leads to the same conclusion. However, the f_0 -meson is not a pure $s\bar{s}$ state as is, for instance, obvious from the decay widths for $J/\Psi \rightarrow f_0\omega$ and $J/\Psi \rightarrow f_0\phi$. This fact is interpreted as f_0 - $\sigma(500)$ mixing. Detailed phenomenological analyses of f_0 - σ mixing in various decay processes [11–14] revealed two ranges for the mixing angle, φ ,

$$(25-40)^\circ \quad (140-165)^\circ \quad (1)$$

A light scalar glueball may affect this result [11].

As an alternative to the quark-antiquark interpretation other authors [15,16] have suggested a tetraquark configuration for the f_0 -meson. This appears as a natural explanation for the fact that the $a_0(980)$ and the f_0 mesons are degenerate in mass and are the heaviest particles of the lightest scalar-meson nonet. For the tetraquark interpretation there seems to be no f_0 - σ mixing [13]. The drawback of this picture is that the two-pion decay of the f_0 is too small as compared to experiment whereas the $a_0 \rightarrow \eta\pi$ is too large. In [17] it has been suggested that the lightest scalar-meson nonet, considered as tetraquarks states, mixes with the scalar-meson nonet with masses around 1200 MeV under the effect of the instanton force. The latter nonet is believed to have a predominant $q\bar{q}$ structure. This mixing leads to a better description

^a e-mail: kroll@physik.uni-wuppertal.de

of the light scalar-meson decays. The f_0 may also have a substantial $K\bar{K}$ molecule component [18]. It goes without saying that the real f_0 -meson is a superposition of all these configurations.

The goal of the present paper is the calculation of the $\gamma^* - f_0$ transition form factors at large photon virtualities. For this calculation the pQCD framework developed by Brodsky and Lepage [19] is utilized in which the process is factorized in a perturbatively calculable hard subprocess (here $\gamma^* \gamma^* \rightarrow q\bar{q}$) and a soft hadronic matrix element, parametrized as a light-cone wave function, which is under control of soft, long-distance QCD. As any hadron the f_0 -meson possesses a Fock decomposition [20] starting with the simple quark-antiquark components

$$|f_0; p\rangle = \sum_{\beta} \int [d\tau]_2 [d^2\mathbf{k}_{\perp}]_2 \Psi_{2,\beta}(\tau, \mathbf{k}_{\perp}) |q\bar{q}, \beta; k_1, k_2\rangle + \text{higher Fock states} \quad (2)$$

where $\Psi_{2,\beta}$ is the light-cone wave function of the $q\bar{q}$ Fock state; the index β labels its decomposition in flavor, color and helicity. The integration measures are defined by

$$[d\tau]_2 = d\tau_1 d\tau_2 \delta(1 - \tau_1 - \tau_2), \\ [d^2\mathbf{k}_{\perp}]_2 = \frac{d^2\mathbf{k}_{\perp 1} d^2\mathbf{k}_{\perp 2}}{16\pi^3} \delta^{(2)}(\mathbf{k}_{\perp 1} + \mathbf{k}_{\perp 2} - \mathbf{p}_{\perp}). \quad (3)$$

In the photon-photon interactions at large photon virtualities the f_0 -meson is generated through its lowest Fock components, mainly the $s\bar{s}$ one. As can be shown [19] the hard generation of the f_0 through higher Fock components is suppressed by inverse powers of the photon virtuality and is therefore neglected. Once the meson is produced it gets dressed by fluctuations into higher Fock components under the effect of long-distance QCD. The calculation of the $\gamma^* - f_0$ transition form factors is similar to the one of the photon-pseudoscalar-meson form factors [19]. The latter calculation is to be generalized in such a way that also hadrons with non-zero orbital angular between their constituents can be treated.

The paper is organized as follows: In the next section the spin part of the light-cone wave function, termed the spin wave function, of the f_0 is constructed assuming that this mesons is an $s\bar{s}$ state. In Sect. 2.1 the collinear reduction of the spin wave function is discussed and, in Sect. 2.2, an example of a light-cone wave function of the f_0 is introduced and compared to the twist-2 and 3 distribution amplitudes. The $\gamma^* - f_0$ transition form factors are defined in Sect. 3.1, followed by a LO perturbative calculation within the modified perturbative approach in which quark transverse degrees of freedom are retained (Sect. 3.2). Numerical results for the form factors in the real-photon limit are given in Sect. 4.1 and compared to the BELLE data. Some comments on the

behavior of the $\gamma^* - f_0$ form factors are presented in Sect. 4.2. Finally, the summary will be given in Sect. 5.

2 The spin wave function of the f_0 -meson

For the description of the hadron the light-cone approach is used which enables one to completely separate the dynamical and kinematical features of the Poincaré invariance [21, 22]. The overall motion of the hadron is decoupled from the internal motion of the constituents, i.e. the light-cone wave function of the hadron, Ψ , is independent of the hadron's momentum and is invariant under the kinematical Poincaré transformations (boosts along and rotations around the 3-directions as well as transverse boosts). Hence, Ψ is determined if it is known at rest. The $s\bar{s}$ Fock component given in (2), is split in a spin part (hereafter denoted spin wave function) and a reduced light-cone wave function, Ψ_0 , which represents the full, soft wave function, Ψ , with a factor K^μ removed from it. As discussed in detail in Ref. [23] the covariant spin wave function can be constructed starting from the observation [24] that, in zero binding energy approximation, an equal-time hadron state (in the spin basis) in the constituent center-of-mass frame equals the (helicity) light-cone state at rest. Consequently, one can use the standard ls coupling scheme in order to couple quark and antiquark to a state of given spin and parity. On boosting the results to a frame with arbitrary hadron momentum one easily reads off the covariant spin wave function.¹

Since the $f_0(980)$ -meson is a $J^{PC} = 0^{++}$ state the quark and antiquark have to couple in a spin-1 state and one unit of orbital angular momenta is required.² The ls coupling scheme leads to the following ansatz for the spin wave function of a final state meson in its rest frame [23, 25] ($\bar{S}_0 = \gamma_0 S^\dagger \gamma_0$):

$$\bar{S}_0 = \sum_{m, \mu_1, \mu_2} k \sqrt{4\pi} Y_{1m}^*(\mathbf{k}/k) \begin{pmatrix} 1/2 & 1/2 & 1 \\ \mu_1 & \mu_2 & \mu_s \end{pmatrix} \begin{pmatrix} 1 & 1 & 0 \\ \mu_s & m & 0 \end{pmatrix} \\ \times v(\hat{p}_2, \mu_2) \bar{u}(\hat{p}_1, \mu_1). \quad (4)$$

Note that μ_1, μ_2 denote spin components and v, \bar{u} are equal-t spinors here. In the meson's rest frame the meson and the constituent momenta read

$$\hat{p}^\mu = (M_0, \mathbf{0}), \quad \hat{p}_1^\mu = (m_1, \mathbf{k}), \quad \hat{p}_2^\mu = (m_2, -\mathbf{k}), \quad (5)$$

where \mathbf{k} is the three-momentum part of the relative momentum of quark and antiquark

$$\mathbf{k} = \frac{1}{2}(\hat{\mathbf{p}}_1 - \hat{\mathbf{p}}_2). \quad (6)$$

¹ In [23] this method has been applied for instance in a calculation of the $\pi - a_1(1260)$ form factors.

² In spectroscopy notation the valence Fock component of f_0 -meson is a 3P_0 state.

In order to retain a covariant formulation, the four-vector $K = (0, \mathbf{k})$ is introduced.³ As is customary in the parton model, the binding energy is neglected and the constituents are considered as quasi-on-shell particles. That possibly crude approximation can be achieved by putting the minus components of the constituents to zero. Hence, $k_3 = 0$ and our relative vector reduces to

$$K = [00\mathbf{k}_\perp]. \quad (7)$$

In this case the spin wave function (4) reads

$$\bar{S}_0 = \frac{1}{\sqrt{2}}[k_{\perp+}v(\hat{p}_2, +)\bar{u}(\hat{p}_1, +) - k_{\perp-}v(\hat{p}_2, -)\bar{u}(\hat{p}_1, -)] \quad (8)$$

where $k_{\perp\pm} = k_{\perp 1} \pm ik_{\perp 2}$. This spin wave function is of the same type as is discussed in [26] for the $l = 1$ Fock components of ρ and π -mesons.

In the infinite momentum frame (IMF), obtained by boosting the meson rest frame momenta along the 3-direction, $p \cdot K = 0$ holds and the quark and antiquark momenta are parametrized as⁴

$$p_1 = \tau p + K, \quad p_2 = \bar{\tau} p - K \quad (9)$$

where $\bar{\tau} = 1 - \tau$ and

$$\begin{aligned} p_1^2 &= m_1^2 = \tau^2 M_0^2 + \mathcal{O}(k_\perp^2), \\ p_2^2 &= m_2^2 = \bar{\tau}^2 M_0^2 + \mathcal{O}(k_\perp^2). \end{aligned} \quad (10)$$

The boost to the IMF leads to

$$\bar{S}_0 = \frac{1}{\sqrt{2}} \left[\frac{2\xi}{1-\xi^2} \frac{k_\perp^2}{M_0} \not{p} - 2 \frac{k_\perp^2}{1-\xi^2} + i\sigma^{\mu\nu} p_\mu K_\nu + M_0 \not{K} \right]. \quad (11)$$

For convenience the variable $\xi = 1 - 2\tau$ is introduced. For $\xi = 0$ this covariant spin wave function coincides with the one employed for the χ_{c0} in [28]. The normalization of the spin wave function is chosen such that

³ As discussed in [23] each unit of orbital angular momentum will be represented by

$$K_\perp^\mu = K^\mu - \hat{v} \cdot K \hat{v}^\mu$$

where $\hat{v}^\mu = \hat{p}^\mu/M_0 = (1, \mathbf{0})$ is the velocity 4-vector. In the rest frame clearly $K_\perp \rightarrow (0, \mathbf{k})$ and one has the appropriate object transforming as a 3-vector under $O(3)$. Thus, K^μ introduced in the line after (6), is strictly speaking K_\perp^μ .

⁴ In [27] the parton momenta are parametrized as

$$p_1 = \tau p + K + \frac{k_\perp^2}{2\tau p \cdot \bar{p}} \bar{p}, \quad p_2 = \bar{\tau} p - K + \frac{k_\perp^2}{2\bar{\tau} p \cdot \bar{p}} \bar{p}$$

where \bar{p} is a light-like vector whose 3-component points in the opposite direction of \mathbf{p} . For this parametrization momentum conservation only holds up to corrections of order k_\perp^2/p . It, however, also leads to the spin wave function (11) up to corrections of order k_\perp^3/M_0 .

$$\text{Tr}(S_0^\dagger S_0) = 4E^2 k_\perp^2 + \mathcal{O}(k_\perp^4) \quad (12)$$

where E is the meson's energy. The meson's $s\bar{s}$ Fock state (2) explicitly reads

$$\begin{aligned} \langle f_0; p | &= \frac{\delta_{c\bar{c}}}{2\sqrt{N_c}} \int \frac{d\xi d^2 k_\perp}{16\pi^3} \Psi_0(\xi, k_\perp^2) \\ &\times \bar{S}_0(s_c; p_1, \lambda_1 | \bar{s}_{\bar{c}}; p_2, \lambda_1 |. \end{aligned} \quad (13)$$

The number of colors is denoted by N_c and c, \bar{c} are color labels. Proper state normalization requires the condition

$$\frac{1}{2} \int \frac{d\xi d^2 k_\perp}{16\pi^3} k_\perp^2 |\Psi_0(\tau, k_\perp^2)|^2 = P_{f_0} \leq 1 \quad (14)$$

where P_{f_0} is the probability of the $s\bar{s}$ Fock component.

2.1 Collinear reduction

In collinear approximation the limit $k_\perp \rightarrow 0$ in the hard subprocess is to be taken in general. However, terms $\propto K^\alpha$ in it combine with terms linear in K in the spin wave function and therefore survive the k_\perp -integration of the wave function. These terms are in general of the same order as the other terms in the spin wave function and it is therefore unjustified to neglect these terms.⁵ Consider the expansion of the subprocess amplitude with respect to K :

$$\mathcal{M} = A_0(\xi) + K^\alpha A_{1\alpha}(\xi) + \mathcal{O}(K^\alpha K^\beta) \quad (15)$$

where A_0 is of order 1 while A_1 is of order $1/p^+$ for dimensional reason. The k_\perp -integration yields

$$\int \frac{d^2 k_\perp}{16\pi^3} \Psi_0(\xi, k_\perp^2) \not{K} \mathcal{M} = -\frac{1}{2} g_\perp^{\nu\alpha} \gamma_\nu A_{1\alpha} \int \frac{dk_\perp^2}{16\pi^2} k_\perp^2 \Psi_0. \quad (16)$$

Formally this is equivalent to the replacement

$$\not{K} \Rightarrow -\frac{k_\perp^2}{2} g_\perp^{\nu\alpha} \gamma_\nu \frac{\partial}{\partial K_\nu} \Big|_{K \rightarrow 0}. \quad (17)$$

The transverse metric tensor is defined by $g_\perp^{11} = g_\perp^{22} = -1$, while all other components are zero in a frame where the meson moves along the 3-direction. In the collinear limit the spin wave function becomes

$$\begin{aligned} \bar{S}_0^{\text{coll}} &= \frac{k_\perp^2}{\sqrt{2}} \left[\frac{2\xi}{1-\xi^2} \frac{\not{p}}{M_0} - \frac{2}{1-\xi^2} \right. \\ &\quad \left. - \frac{1}{2} (i\sigma_{\mu\alpha} p^\mu + M_0 \gamma_\alpha) g_\perp^{\alpha\beta} \frac{\partial}{\partial K_\beta} \right]_{K \rightarrow 0}. \end{aligned} \quad (18)$$

Multiplying the spin wave function with the reduced wave function and integrating over k_\perp , one arrives at the associated

⁵ For $l = 0$ hadrons these terms are suppressed by k_\perp^2 ; the leading term is k_\perp -independent.

distribution amplitudes. The first term in (18) generates the twist-2 distribution amplitude

$$\frac{\bar{f}_0}{2\sqrt{2N_c}}\Phi_0(\xi) = \frac{2\xi}{1-\xi^2} \int \frac{dk_\perp^2}{16\pi^2} \frac{k_\perp^2}{M_0} \Psi_0. \quad (19)$$

Because of charge conjugation invariance the twist-2 distribution amplitude is antisymmetric in ξ . It possesses the Gegenbauer expansion and depends on the factorization scale, μ_F [12, 29, 30],

$$\Phi_0(\xi, \mu_F) = \frac{N_c}{2}(1-\xi^2) \sum_{m=1,3,\dots} B_m(\mu_F) C_m^{3/2}(\xi). \quad (20)$$

Evidently, the reduced wave function must be symmetric in ξ . The Gegenbauer coefficients in (20), which encode the soft, non-perturbative QCD, evolve with the factorization scale as

$$B_m(\mu_F) = B_m(\mu_0) \left(\frac{\alpha_s(\mu_0)}{\alpha_s(\mu_F)} \right)^{-\gamma_m/\beta_0} \quad (21)$$

where

$$\gamma_m = C_F \left(1 - \frac{2}{(m+1)(m+2)} + 4 \sum_{j=2}^{m+1} \frac{1}{j} \right). \quad (22)$$

Here, $\beta_0 = (11N_c - 2n_f)/3$, $C_F = 4/3$ and n_f denotes the number of active flavors. For the initial scale, μ_0 , the value 1.41 GeV is chosen in this article. The decay constant \bar{f}_0 depends on the scale too [12]

$$\bar{f}_0(\mu_F) = \bar{f}_0(\mu_0) \left(\frac{\alpha_s(\mu_0)}{\alpha_s(\mu_F)} \right)^{4/\beta_0}. \quad (23)$$

The other terms in (18) are of twist-3 nature although they do not correspond to the full twist-3 contributions since, in general, they also receive contributions from a second reduced wave function. This is, however, of no relevance for the purpose of the present paper, namely the calculation of the $\gamma^* - f_0$ transition form factors. As we shall see in the following there is no twist-3 contribution to it. Anyway the k_\perp -integration of the other terms leads to two further distribution amplitudes which are related to Φ_0 in the case at hand:

$$\begin{aligned} \Phi_{0s}(\xi, \mu_F) &= \frac{1}{\xi} \Phi_0(\xi, \mu_F), \\ \Phi_{0\sigma}(\xi, \mu_F) &= \frac{1-\xi^2}{4\xi} \Phi_0(\xi, \mu_F). \end{aligned} \quad (24)$$

Both these distribution amplitudes are symmetric in ξ and only the even terms appear in their Gegenbauer expansions.

With the help of these distribution amplitudes one can transform the product of wave function and collinear spin wave function (18), integrated over k_\perp , into the form

$$\begin{aligned} &\int \frac{d^2k_\perp}{16\pi^3} \Psi_0(\xi, k_\perp^2) \bar{S}_0^{\text{coll}} \\ &= \frac{\bar{f}_0}{2\sqrt{2N_c}} \frac{1}{\sqrt{2}} \left[\Phi_0 \not{p} - \Phi_{0s} M_0 \right. \\ &\quad \left. - \Phi_{0\sigma} M_0 (i\sigma_{\mu\alpha} p^\mu + M_0 \gamma_\alpha) g_\perp^{\alpha\beta} \frac{\partial}{\partial K_\beta} \right]_{K \rightarrow 0}. \end{aligned} \quad (25)$$

This expression resembles the corresponding pion spin wave function to twist-3 accuracy [31, 32].

2.2 A wave function for the f_0 meson

For the evaluation of the transition form factors the light-cone wave function is to be specified. It is modeled as a Gaussian in $k_\perp^2/(1-\xi^2)$ times the most general ξ dependence

$$\Psi_0 = c \sum_{n=0,2,\dots} \tilde{B}_n C_n^{3/2}(\xi) \exp \left[-4 \frac{a_0^2 k_\perp^2}{1-\xi^2} \right] \quad (26)$$

with

$$c = 16\pi^2 \sqrt{2N_c} \bar{f}_0 M_0 a_0^4. \quad (27)$$

This wave function is similar to the one for the pion advocated for in [20]. It has been used for instance in the calculation of the photon–pseudoscalar transition form factors [33] or in the analysis of pion electroproduction [34]. Insertion of the wave function into Eq. (19) leads to the associated distribution amplitude (20) with the Gegenbauer coefficients (m is an odd integer)

$$B_m = \frac{m}{2m+1} \tilde{B}_{m-1} + \frac{m+3}{2m+5} \tilde{B}_{m+1}. \quad (28)$$

As a consequence of charge conjugation invariance which forces Ψ_0 to be symmetric in ξ , the matrix element

$$\langle f_0; p | \bar{s}(0) \gamma_\mu s(0) | 0 \rangle = \frac{\sqrt{N_c}}{2} \int d\xi \frac{dk_\perp^2}{16\pi^2} \Psi_0 \text{Tr}[\bar{S}_0 \gamma_\mu] \quad (29)$$

vanishes in accord with the result quoted in [12]. On the other hand, the scalar density provides

$$\langle f_0; p | \bar{s}(0) s(0) | 0 \rangle = M_0 \bar{f}_0 = \frac{\sqrt{N_c}}{2} \int d\xi \frac{dk_\perp^2}{16\pi^2} \Psi_0 \text{Tr}[\bar{S}_0]. \quad (30)$$

Evaluation of the integral leads to $\bar{B}_0 \simeq -1$. This estimate is to be taken with caution since Φ_{0s} in (24) is likely not the full twist-3 distribution amplitude, but it provides orientation. As is obvious from the vacuum-particle matrix element of quark field operators given in (30), the decay constant is a short-distance quantity; it represents the wave function at the origin of the configuration space. It is also clear that only the $s\bar{s}$ Fock component of the f_0 -meson contributes to this matrix element.

For the numerical evaluation of the $\gamma^* - f_0$ transition form factors the wave function will be restricted to the first Gegenbauer term, all others are neglected. We have

$$\psi_{01} = 3cB_1 \exp \left[-4 \frac{a_0^2 k_\perp^2}{1 - \xi^2} \right] \quad (31)$$

with

$$B_1 \simeq \tilde{B}_0/3 \simeq -1/3. \quad (32)$$

In this case the twist-2 distribution amplitude reads

$$\Phi_{01} = \frac{N_c}{2} (1 - \xi^2) B_1 C_1^{3/2}(\xi). \quad (33)$$

For the transverse-size parameter, a_0 , the value 0.8 GeV^{-1} is taken in the following. This value is very close to the corresponding value for the pion; see [33]. The r.m.s. k_\perp is related to the transverse-size parameter by

$$\sqrt{\langle k_\perp^2 \rangle} = \sqrt{\frac{3}{14}} \frac{1}{a_0}. \quad (34)$$

For the value $a_0 = 0.8 \text{ GeV}^{-1}$ the r.m.s. value of k_\perp is 0.58 GeV which is similar to the corresponding results for the valence Fock components of other hadrons. For the decay constant the value

$$\tilde{f}_0(\mu_0) = (180 \pm 15) \text{ MeV} \quad (35)$$

is adopted, which has been derived by De Fazio and Pennington [35] from radiative $\phi \rightarrow f_0 \gamma$ decays with the help of QCD sum rules (see also [36]). In [35] the f_0 -meson is considered as a (dominantly) $s\bar{s}$ state. The value (35) is extracted from the stability window for the Borel parameter between 1.2 and 2 GeV^2 . This is consistent with the initial scale chosen in this article.

3 The $\gamma^* - f_0$ transition form factors

3.1 The definition of the form factors

Let us consider the general case of two virtual photons

$$\gamma^*(q_1, \lambda_1) + \gamma^*(q_2, \lambda_2) \rightarrow f_0(p) \quad (36)$$

where q_i and p denote the momenta of the photons and the mesons while λ_i are the helicities of the photons. One has

$$q_1^2 = -Q_1^2, \quad q_2^2 = -Q_2^2, \quad p^2 = M_0^2. \quad (37)$$

It is convenient to introduce the following variables [37]:

$$\overline{Q}^2 = \frac{1}{2}(Q_1^2 + Q_2^2), \quad \omega = \frac{Q_1^2 - Q_2^2}{Q_1^2 + Q_2^2} \quad (38)$$

where, obviously, $-1 \leq \omega \leq 1$.

The transition vertex is defined by the matrix element of the time-ordered product of two electromagnetic currents,

$$\Gamma^{\mu\nu} = -ie_0^2 \int d^4x e^{-iq_1x} \langle f_0; p | T \{ j_{\text{em}}^\mu(x) j_{\text{em}}^\nu(0) \} | 0 \rangle \quad (39)$$

where

$$j_{\text{em}}^\mu = e_u \bar{u}(x) \gamma^\mu u(x) + e_d \bar{d}(x) \gamma^\mu d(x) + e_s \bar{s}(x) \gamma^\mu s(x) \quad (40)$$

and e_i are the quark charges in units of the positron charge, e_0 . Following [5] the vertex is covariantly decomposed as

$$\begin{aligned} \Gamma^{\mu\nu} = ie_0^2 \frac{q_1 \cdot q_2}{M_0} \left\{ \left[-g^{\mu\nu} + \frac{1}{\overline{Q}^4 \kappa} [q_1 \cdot q_2 (q_1^\mu q_2^\nu + q_2^\mu q_1^\nu) \right. \right. \\ \left. \left. + Q_1^2 q_2^\mu q_2^\nu + Q_2^2 q_1^\mu q_1^\nu] \right] F_T(\overline{Q}^2, \omega) \right. \\ \left. - \frac{q_1 \cdot q_2}{\overline{Q}^4 \kappa} \left[q_1^\mu + \frac{Q_1^2}{q_1 \cdot q_2} q_2^\mu \right] \left[q_2^\nu + \frac{Q_2^2}{q_1 \cdot q_2} q_1^\nu \right] \right. \\ \left. \times F_L(\overline{Q}^2, \omega) \right\} \end{aligned} \quad (41)$$

where

$$\kappa = \frac{(q_1 \cdot q_2)^2}{\overline{Q}^4} - 1 + \omega^2 = \omega^2 + \frac{M_0^2}{\overline{Q}^2} + \frac{M_0^4}{4\overline{Q}^4} \quad (42)$$

and e_0 denotes the positron charge. Current conservation is manifest:

$$q_{1\mu} \Gamma^{\mu\nu} = 0, \quad q_{2\nu} \Gamma^{\mu\nu} = 0. \quad (43)$$

As one sees from (41) there are two form factors, one for transverse photon polarization, F_T , and another one for longitudinal polarization, F_L . By definition the form factors are dimensionless.

Contracting the vertex function with the polarization vectors of the photons and using transversality ($\epsilon_i q_i = 0$), one arrives at

$$\begin{aligned} \epsilon_1^\mu \epsilon_2^\nu \Gamma_{\mu\nu} = ie_0^2 \frac{q_1 \cdot q_2}{M_0} \left\{ \left[-\epsilon_1 \cdot \epsilon_2 + \frac{q_1 \cdot q_2}{\kappa \overline{Q}^4} \epsilon_1 \cdot q_2 \epsilon_2 \cdot q_1 \right] F_T \right. \\ \left. - \frac{1 - \omega^2}{\kappa q_1 \cdot q_2} \epsilon_1 \cdot q_2 \epsilon_2 \cdot q_1 F_L \right\}. \end{aligned} \quad (44)$$

One can show, most easily in the equal-energy brick wall frame (see Fig. 1), defined by

$$q_1 = (v \ 0 \ 0 \ a_1), \quad q_2 = (v \ 0 \ 0 \ a_2), \quad p = (2v \ 0 \ 0 \ a_1 + a_2), \quad (45)$$

that the contraction with transverse photon polarization vectors with the same helicity projects out the form factor F_T and with longitudinal ones F_L :

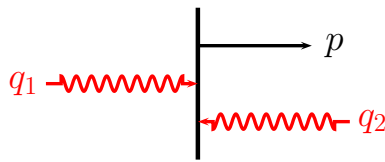


Fig. 1 The equal-energy brick wall frame

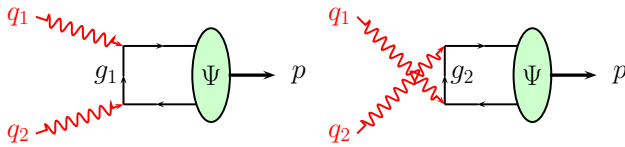


Fig. 2 LO Feynman graphs for the $\gamma^* \rightarrow f_0$ transition form factors. The momenta of the virtual partons are denoted by g_1 and g_2

$$\begin{aligned}\epsilon_1^\mu(\lambda_1)\epsilon_2^\nu(\lambda_2)\Gamma_{\mu\nu} &= -ie_0^2 \frac{q_1 \cdot q_2}{M_0} F_T(\bar{Q}^2, \omega) \delta_{\lambda_1 \lambda_2}, \\ \epsilon_1^\mu(0)\epsilon_2^\nu(0)\Gamma_{\mu\nu} &= ie_0^2 \sqrt{1-\omega^2} \frac{\bar{Q}^2}{M_0} F_L(\bar{Q}^2, \omega).\end{aligned}\quad (46)$$

If the photons have different helicities the vertex function is zero.

3.2 The LO perturbative calculation

In the perturbative calculation of the form factors, performed at large \bar{Q}^2 , the mass of the f_0 -meson is neglected whenever this is possible. From the Feynman graphs shown in Fig. 2 one finds for the vertex function (39)

$$\begin{aligned}\Gamma_{\mu\nu} &= -i \frac{1}{2} e_0^2 e_s^2 \sqrt{N_c} \int \frac{d\xi d^2 k_\perp}{16\pi^3} \Psi_0(\xi, k_\perp) \\ &\times \left\{ \text{Tr} \left[\bar{S}_0 \gamma_\mu \frac{\frac{1}{2}(1-\xi)\not{p} + \not{K} - q_1}{g_1^2} g_1^\nu \gamma_\nu \right] \right. \\ &\left. + \text{Tr} \left[\bar{S}_0 \gamma_\nu \frac{\frac{1}{2}(1-\xi)\not{p} + \not{K} - q_2}{g_2^2} \gamma_\mu \right] \right\}\end{aligned}\quad (47)$$

where the parton virtualities read (see also Fig. 2)

$$g_1^2 = -\bar{Q}^2(1+\xi\omega) - k_\perp^2, \quad g_2^2 = -\bar{Q}^2(1-\xi\omega) - k_\perp^2. \quad (48)$$

Taking into consideration that the traces are only non-zero for even numbers of γ matrices, one notices that only the first term of the spin wave function (11), i.e. the leading-twist piece, contributes to the traces. The twist-3 terms lead to an odd number of γ matrices in the traces, the fourth term is neglected. With the help of (46) one finally arrives at the following expressions for the form factors:

$$\begin{aligned}F_T(\bar{Q}^2, \omega) &= -4\sqrt{2N_c} \frac{e_s^2}{\bar{Q}^2} \frac{\omega^2 + \frac{1}{2}\frac{M_0^2}{\bar{Q}^2}}{1 + \frac{1}{2}\frac{M_0^2}{\bar{Q}^2}} \\ &\times \int \frac{d\xi dk_\perp^2}{16\pi^2} k_\perp^2 \Psi_0(\xi, k_\perp) \\ &\times \frac{\xi^2}{1-\xi^2} \frac{1}{1-\xi^2\omega^2 + 2k_\perp^2/\bar{Q}^2}, \\ F_L(\bar{Q}^2, \omega) &= -\frac{1}{2} \frac{M_0^2}{\bar{Q}^2} \frac{1 + \frac{1}{2}\frac{M_0^2}{\bar{Q}^2}}{\omega^2 + \frac{1}{2}\frac{M_0^2}{\bar{Q}^2}} F_T(\bar{Q}^2, \omega).\end{aligned}\quad (49)$$

Because of the variation of ω^2 between 0 and 1 the mass dependent terms in front of the integral are kept. For $\omega \rightarrow \pm 1$ they exactly cancel whereas for $\omega \rightarrow 0$ $F_T \propto \bar{Q}^{-4}$. The wave function (26) generates a factor $(1-\xi^2)^2$ in the k_\perp^2 integration. Hence, there is no singularity at the end points $\xi \rightarrow \pm 1$ for all ω . One also notices from (49) that

$$F_{T,L}(\bar{Q}^2, -\omega) = F_{T,L}(\bar{Q}^2, \omega). \quad (50)$$

For $\omega \gg M_0^2/(2\bar{Q}^2)$ the terms $\sim M_0^2/\bar{Q}^2$ in (49) can be neglected and

$$F_T \propto 1/\bar{Q}^2, \quad F_L \propto 1/\bar{Q}^4. \quad (51)$$

For $\omega \rightarrow 0$, on the other hand, only the term $\sim M_0^2/(2\bar{Q}^2)$ remains and

$$F_{T,L} \propto 1/\bar{Q}^4. \quad (52)$$

Explicitly, for $\omega \rightarrow 1$ (i.e. $Q_1^2 = 0$)

$$\begin{aligned}F_T(Q_1^2, 1) &= -8\sqrt{2N_c} \frac{e_s^2}{Q_1^2} \int \frac{d\xi dk_\perp^2}{16\pi^2} k_\perp^2 \Psi_0(\xi, k_\perp) \\ &\times \frac{\xi^2}{1-\xi^2} \frac{1}{1-\xi^2 + 4k_\perp^2/Q_1^2}.\end{aligned}\quad (53)$$

For a wave function of the type (26) one can write Eq. (53) as

$$F_T(Q_1^2, 1) = \varrho(a_0^2 Q_1^2) F_T^{\text{coll}}(Q_1^2, 1) \quad (54)$$

with

$$\begin{aligned}F_T^{\text{coll}} &= -2 \frac{e_s^2}{Q_1^2} \bar{f}_0 M_0 \int d\xi \frac{\xi \Phi_0(\xi)}{1-\xi^2} \\ &= -2N_c \frac{e_s^2}{Q_1^2} \bar{f}_0 M_0 \sum_{m=1,3,\dots} B_m\end{aligned}\quad (55)$$

and

$$\varrho(x) = \int dK \frac{K e^{-K}}{1 + K/x}. \quad (56)$$

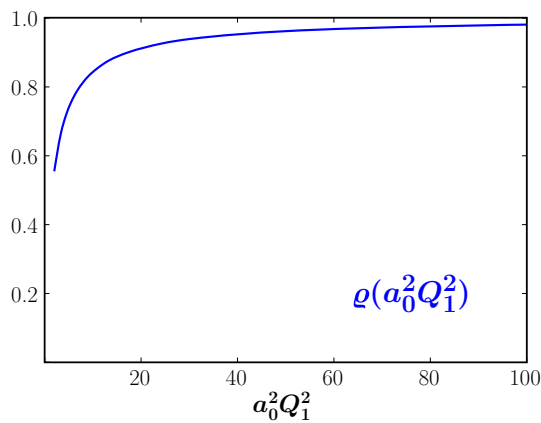


Fig. 3 The reduction function ρ versus $a_0^2 Q_1^2$

For this type of wave functions the transition form factor is given by the collinear result multiplied by a universal reduction factor ρ . The latter function is shown in Fig. 3. It is interesting that, in the collinear approximation, the LO perturbative result for the form factor is related to the sum over all Gegenbauer coefficients. The $\gamma - \pi$ transition form factor possesses this property too. This makes it clear that it is impossible to extract more than one Gegenbauer coefficient from the $\gamma - f_0$ transition form factor data. This coefficient is to be regarded as an effective one. NLO corrections may allow one to fix a second coefficient [37]. The situation improves for $|\omega| < 1$ as will be discussed in Sect. 4.2.

4 Results

4.1 The real-photon limit

The BELLE collaboration [1] extracted the $\gamma - f_0$ transition form factor from the cross sections on $\gamma^* \gamma \rightarrow \pi^0 \pi^0$. In order to fix the normalization of that form factor the couplings of the f_0 to both the two-photon and the $\pi\pi$ channels are required. These two couplings are not well known [10]. Hence, the normalization of the $\gamma - f_0$ transition form factor is subject to considerable uncertainties. The published data on the transition form factor, $F_T(Q_1^2)$, are scaled by the value of the form factor at $Q_1^2 = 0$ obtained from the width of the two-photon decay of the f_0 -meson ($M_0 = (990 \pm 20)$ MeV [10])

$$\Gamma(f_0 \rightarrow \gamma\gamma) = \frac{\pi}{4} \alpha_{\text{em}}^2 M_0 |F_T(0)|^2. \quad (57)$$

From the average decay width quoted in [10], one obtains

$$|F_T(0)| = 0.0865 \pm 0.0141. \quad (58)$$

The BELLE collaboration uses the slightly different value $|F_T(0)|_{\text{BELLE}} = 0.0832 \pm 0.0136$.

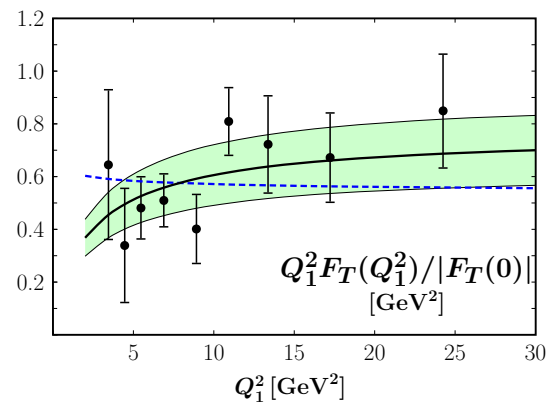


Fig. 4 The Q_1^2 -dependence of the $\gamma - f_0$ transition form factor scaled by $|F_T(0)|/Q_1^2$ (for $|F_T(0)|$ the value (58) is taken). Data are taken from [1]; only the statistical errors are shown. The dashed and solid lines are the results of the collinear approximation and the modified perturbative approach evaluated from wave function (31), respectively. The shaded band represents the normalization uncertainty of the second result

In a first step the BELLE data are compared to the collinear result (55) for F_T . For the factorization scale $\mu_F^2 = Q_1^2$ is used and for Λ_{QCD} the value 180 MeV in combination with four flavors. Allowing only for the first Gegenbauer term in the expansion (20) of Φ_0 and taking for the decay constant the value (35), we fit B_1 against the BELLE data. The fit yields $B_1^{\text{coll}}(\mu_0) = -0.44 \pm 0.04$ and $\chi^2 = 10.3$ for 9 data points. The fitted value of B_1 is not far from the estimate quoted in (32). For these wave function parameters the probability of the $s\bar{s}$ Fock component of the f_0 -meson is (see (14)):

$$P_{f_0} = \frac{12}{5} N_c [\pi \bar{f}_0 M_0 a_0^2 B_1]^2 = 0.18. \quad (59)$$

The results of the fit are shown in Fig. 4. Reasonable agreement with experiment is to be seen within rather large errors although the shape of the fit is opposite to that of the data: the collinear result for the scaled form factor, $Q_1^2 F_T^{\text{coll}}$ slightly decreases with increasing Q_1 due to the evolution of the decay constant and the Gegenbauer coefficient, B_1 , whereas the data increase in tendency.

An increasing scaled form factor can be generated by quark transverse momenta in the hard scattering kernel and in the wave function, see Fig. 3. Retaining the quark transverse momenta implies that quarks and antiquarks are pulled apart in the transverse configuration or impact-parameter space. The separation of color sources is accompanied by the radiation of gluons. These radiative corrections have been calculated in Ref. [38] in the form of a Sudakov factor in the impact parameter plane. The Sudakov factor, e^{-S} , comprises resummed leading and next-to-leading logarithms which are not taken into account by the usual QCD evolution. The k_\perp -factorization combined with the Sudakov factor is termed the modified perturbative approach (mpa) [38]. It has been used, for instance, in calculations of the pion electromagnetic

form factor [38] or the $\pi\text{--}\gamma$ transition form factor [33] and will be used here as well. In the impact-parameter plane the transition form factor (53) reads

$$F_T(Q_1^2, 1) = -\frac{e_s^2 \sqrt{2N_C}}{2\pi} \int_{-1}^1 d\xi \frac{\xi^2}{1-\xi^2} \int_0^{1/\Lambda_{\text{QCD}}} db b \times [k_\perp^2 \Psi_0] e^{-S} K_0(bQ_1/2\sqrt{1-\xi^2}). \quad (60)$$

The integrand is completed by the Sudakov factor, $\exp(-S)$, its explicit form can be found for instance in [33]. The Sudakov factor provides the sharp cut-off of the b -integral at $1/\Lambda_{\text{QCD}}$. Since $1/b$ in the Sudakov factor marks the interface between the non-perturbative soft momenta which are implicitly accounted for in the meson wave function, and the contributions from soft gluons, incorporated in a perturbative way in the Sudakov factor [33, 38], it naturally acts as the factorization scale. The Bessel function K_0 is the Fourier transform of the hard scattering kernel and $[k_\perp^2 \Psi_0]$ is the Fourier transform of the wave function (31) multiplied by k_\perp^2 . It reads

$$[k_\perp^2 \Psi_0] = \frac{3\pi}{4} \sqrt{2N_C} \bar{f}_0 M_0 B_1 (1-\xi^2)^2 \times \left(1 - \frac{1-\xi^2}{16a_0^2} b^2\right) e^{-\frac{1-\xi^2}{16a_0^2} b^2}. \quad (61)$$

Evaluating the form factor within the modified perturbative approach and fitting B_1 to the BELLE data [1] one arrives at the results shown in Fig. 4. The fit provides the following value for the Gegenbauer coefficient⁶:

$$B_1^{\text{mpa}}(\mu_0) = -0.57 \pm 0.05 \quad (62)$$

and $\chi^2 = 5.9$ for 9 data points. The normalization uncertainty of the theoretical result follows from the errors of B_1 and $F_T(0)$; see (58). The agreement of the result obtained within the modified perturbative approach, with experiment is somewhat better than for the collinear approximation—the scaled form factor increases with Q_1^2 as the data do. This increase is the effect of the k_\perp corrections shown in Fig. 3, the Sudakov factor plays a minor role in this context.⁷ In passing it is noted that the predictions presented in [2] lie markedly below experiment for $Q_1^2 \gtrsim 10 \text{ GeV}^2$.

⁶ As shown for the case of the $\gamma\text{--}\pi$ form factor in [33] the contributions from the higher Gegenbauer terms are suppressed as compared to the lowest one. This property of the modified perturbative approach comes into effect here, too.

⁷ In the analysis of the $\gamma\text{--}f_2$ form factor performed in [6] the collinear factorization framework does also not suffice. In order to achieve fair agreement with experiment [1] soft end-point corrections have to be included in the analysis.

The value (62) of the Gegenbauer coefficient B_1 not far from the QCD sum result [12]:

$$\bar{f}_0(\mu_0) = (410 \pm 22) \text{ MeV}, \quad B_1(\mu_0) = -0.65 \pm 0.07. \quad (63)$$

The coefficient B_3 is found to be zero within errors. However, the value of \bar{f}_0 is substantially larger than the value (35) used in the form factor calculation. More precisely, the fit to the BELLE data fixes the product of \bar{f}_0 and B_1 for which the following results exist:

$$\begin{aligned} \bar{f}_0(\mu_0) B_1(\mu_0) &= (-0.079 \pm 0.007) \text{ GeV} && \text{collinear,} \\ &= (-0.103 \pm 0.990) \text{ GeV} && \text{mpa} \\ &= (-0.267 \pm 0.029) \text{ GeV} && [12]. \end{aligned} \quad (64)$$

The product of \bar{f}_0 and B_1 derived in [12] is substantially larger than the BELLE data [1] on the $\gamma\text{--}f_0$ transition form factors allow. This product of \bar{f}_0 and B_1 is also in conflict with a light-cone wave function interpretation since it leads to a probability larger than 1. Of course a smaller value of the transverse-size parameter would cure this problem for the prize of an implausible compact valence Fock component. For instance, if one halves a_0 the probability is about 0.12 but $\sqrt{\langle k_\perp^2 \rangle} \simeq 1.2 \text{ GeV}$.

The last issue to be discussed is the contribution from the non-strange $q\bar{q}$ Fock state to the $\gamma\text{--}f_0$ transition form factor. This is usually considered as $f_0\text{--}\sigma$ mixing [11–17]. As for the $\eta\text{--}\eta'$ system [39] this mixing is treated in the quark-flavor basis. As a consequence of the smallness of OZI-rule violations $\eta\text{--}\eta'$ mixing is particularly simple in that basis—there is a common mixing angle for the states and the decay constants. It is assumed that this mixing scheme also holds for the case of interest here. Let σ_n and σ_s be states with the lowest Fock components $n\bar{n} = (u\bar{u} + d\bar{d})/\sqrt{2}$ and $s\bar{s}$, respectively. In analogy to (30) the corresponding decay constants are defined by the σ_i -vacuum matrix elements of the quark field operators:

$$\begin{aligned} \langle \sigma_n | \bar{n}(0) n(0) | 0 \rangle &= M_{\sigma_n} \bar{f}_n, \\ \langle \sigma_s | \bar{s}(0) s(0) | 0 \rangle &= M_{\sigma_s} \bar{f}_s. \end{aligned} \quad (65)$$

Since in hard processes only small spatial quark–antiquark separations are of relevance it seems plausible to embed the particle dependence and the mixing behavior of the $q\bar{q}$ Fock components solely into the decay constants⁸ (for a detailed discussion of this procedure in the $\eta\text{--}\eta'$ case see [40]). In generalization of (30) one may also define the decay constants \bar{f}_i^q ($i = f_0, \sigma; q = n, s$)

$$\langle i | \bar{q}(0) q(0) | 0 \rangle = M_i \bar{f}_i^q. \quad (66)$$

⁸ I.e. with the exception of the decay constants, the wave functions of the basis states, σ_n and σ_s , are assumed to be the same.

These decay constants mix according to

$$\begin{aligned}\bar{f}_\sigma^n &= \bar{f}_n \cos \varphi, & \bar{f}_\sigma^s &= -\bar{f}_s \sin \varphi, \\ \bar{f}_0^n &= \bar{f}_n \sin \varphi, & \bar{f}_0^s &= \bar{f}_s \cos \varphi.\end{aligned}\quad (67)$$

Hence, the γ^*-f_0 transition form factors are made of two contributions,

$$F_{T,L} = F_{T,L}^n + F_{T,L}^s \quad (68)$$

where the n and s contributions differ from (49) only by the decay constants, \bar{f}_n and \bar{f}_s , the mixing angle, φ , and the quark charges, $(e_u^2 + e_d^2)/\sqrt{2}$ and e_s^2 . Thus, the contribution from the $n\bar{n}$ Fock state is taken into account if in (49), and in other expressions derived for the form factors, the decay constant, \bar{f}_0 , is to be replaced by an effective one defined by

$$\bar{f}_0^{\text{eff}} = \bar{f}_n \sin \varphi \frac{1}{\sqrt{2}} \frac{e_u^2 + e_d^2}{e_s^2} + \bar{f}_s \cos \varphi. \quad (69)$$

According to [12,41] $\bar{f}_n \simeq \bar{f}_s$. Since the decay constant quoted in (35) is to be identified with \bar{f}_0^s and since $|\cos \varphi|$ is close to 1, see (1), it suffices to assume $\bar{f}_n \simeq \bar{f}_s \simeq \bar{f}_0$ for a rough estimate. For the range $\varphi = (25-40)^\circ$ of the mixing angle quoted in (1) one finds

$$\bar{f}_0^{\text{eff}} / \bar{f}_0 = 2.4-3.0. \quad (70)$$

Clearly, this leads to a transition form factor which is in conflict with the BELLE data [1]. Using the second range of mixing angles in (1) one obtains reasonable agreement with experiment. Particularly favored is the range $\varphi = (145-151)^\circ$ for which the form factor stays within the uncertainty band displayed in Fig. 4. An exact determination of the mixing angle is not possible at present given the poor information available for the basic decay constants, \bar{f}_n , \bar{f}_s , and the assumption on the explicit form of the light-cone wave function.

4.2 The case of two virtual photons

Here, in this subsection, we will comment on the γ^*-f_0 transition form factor. As is the case for $\omega = 1$, the Sudakov factor plays a minor role. In order to estimate the importance of the power corrections taken into account in the modified perturbative approach the ratio of the form factors evaluated from (49) (transformed to the impact parameter plane and with the Sudakov factor included) and from the collinear approximation

$$F_T^{\text{coll}}(\bar{Q}^2, \omega) = -\frac{e_s^2}{\bar{Q}^2} \bar{f}_0 M_0 \frac{\omega^2 + \frac{1}{2} \frac{M_0^2}{\bar{Q}^2}}{1 + \frac{1}{2} \frac{M_0^2}{\bar{Q}^2}} \int d\xi \frac{\xi \Phi_0(\xi)}{1 - \xi^2 \omega^2} \quad (71)$$

is displayed in Fig. 5. As expected the power corrections become smaller with increasing \bar{Q}^2 and their importance

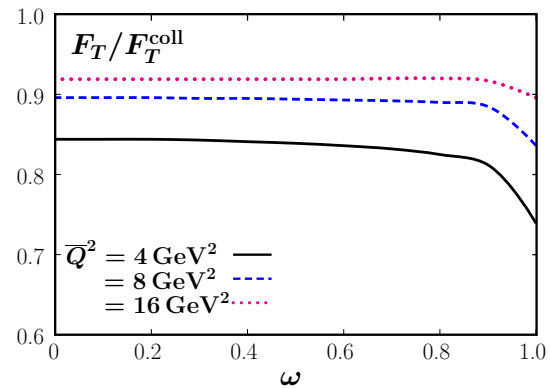


Fig. 5 The ratio of the transition form factors evaluated from (49) and from the collinear result (71) versus ω for a set of \bar{Q}^2 values. The form factors are evaluated from the wave function (31) and the associated distribution amplitude (33), respectively

decreases if ω deviated from 1. The same observation has been made in [37] in the case of the $\gamma^*-\pi$ transition form factor. As noticed in [37] the reason for this effect is the term $1 - \xi^2 \omega^2$ in the hard scattering kernel which controls to which extent the form factor is sensitive to contributions from the end-point regions $\xi \rightarrow \pm 1$ where soft effects can be important.

Since the power corrections are small at small ω , it is of interest to look at the transition form factor (71) in this region. Using the Gegenbauer expansion of the distribution amplitude the integral can be carried out term by term. The full result is a power series in ω^2 leaving aside the ω -dependence of the prefactor. The first terms of this series read

$$\begin{aligned}F_T^{\text{coll}}(\bar{Q}^2, \omega) &= -\frac{2}{5} N_c e_s^2 \frac{\bar{f}_0 M_0}{\bar{Q}^2} \frac{\omega^2 + \frac{1}{2} \frac{M_0^2}{\bar{Q}^2}}{1 + \frac{1}{2} \frac{M_0^2}{\bar{Q}^2}} \\ &\times \left[B_1 + \omega^2 \frac{3}{7} \left(B_1 + \frac{20}{27} B_3 \right) \right. \\ &\left. + \omega^4 \frac{5}{21} \left(B_1 + \frac{40}{33} B_3 + \frac{56}{143} B_5 \right) + \dots \right].\end{aligned}\quad (72)$$

As one notices the m th Gegenbauer coefficient comes with the power ω^{m-1} first. For \bar{Q}^2 larger than 4 GeV² the difference between the modified perturbative approach and the collinear result is smaller than 10%. Hence, the result in the modified perturbative approach, evaluated from the wave function (26), is not far from the collinear result (72). Thus, as is the case for the $\gamma^*-\pi$ transition form factor [37], a measurement of the γ^*-f_0 transition form factors for a range of small ω would therefore provide valuable constraints on the f_0 distribution amplitude.

In Fig. 6 the γ^*-f_0 transition form factor, evaluated from the wave function (31) within the modified perturbative

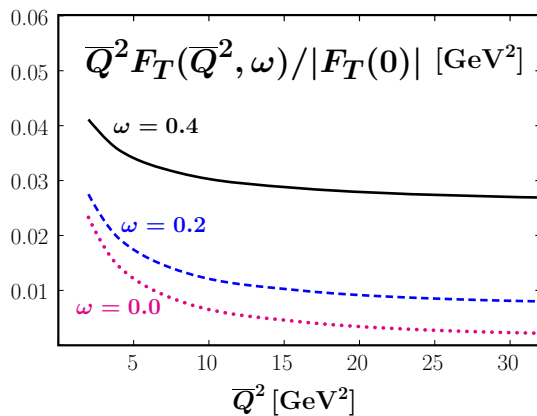


Fig. 6 The γ^*-f_0 transition form factor, scaled by $|F_T(0)|/\overline{Q}^2$, evaluated from the wave function (31) (with $B_1 = -0.57$) within the modified perturbative approach versus \overline{Q}^2 for a set of ω values

approach, is shown for several small values of ω . It is clearly seen that the form factor drops with \overline{Q}^2 increasingly stronger than $1/\overline{Q}^2$ with decreasing ω . At $\omega = 0$ it decreases as $1/\overline{Q}^4$ (aside from evolution logarithms).

5 Summary

In this article the spin wave function of the $f_0(980)$ meson is constructed under the assumption that the meson is dominantly a strange–antistrange quark state. The collinear limit of the spin wave function is also discussed and the connection to the twist-2 and twist-3 distribution amplitudes is made. The spin wave function is applied in a calculation of the γ^*-f_0 transition form factors. In the real-photon limit the results for the transverse form factor are compared to the large momentum-transfer data measured by the BELLE collaboration recently. It turns out that, for the momentum-transfer range explored by BELLE, the collinear approximation does not suffice, power corrections to it, modeled as quark transverse moment effects, seem to be needed. The parameters required in this calculation in order to achieve agreement with BELLE form factor data, the transverse-size parameter, a_0 , the decay constant, \tilde{f}_0 , and the lowest (effective) Gegenbauer coefficient, B_1 , have plausible values. However, Cheng et al. [12] in their analysis of charmless B -meson decays, adopt a much larger value for \tilde{f}_0 than (35). It remains to be seen whether the B -meson decays can be reconciled with the decay constant (35). The implications of σ – f_0 mixing for the transition form factors are also briefly discussed. A mixing angle of about 150° seems to be favored. The paper is completed by presenting results on the γ^*-f_0 form factors and on their collinear limits. It turns out that, in many aspects, the photon f_0 form factors have properties similar to the form factors for the transition from a photon to

the π^0 or other pseudoscalar mesons. However, the limits for $Q_1^2 \rightarrow \infty$ are different. Whereas for the pseudoscalar mesons the limits of the scaled form factors are finite (e.g. $Q_1^2 F_{\gamma\pi^0} \rightarrow \sqrt{2}f_\pi$) the γ – f_0 form factor F_T tends to zero $\sim f_0(\mu_0)B_1(\mu_0)(\alpha_s(\mu_0)/\alpha_s(Q_1^2))^{-4/25}$. The γ^*-f_0 transition form factors also play a role in the calculation of the hadronic light-by-light contribution to the muon anomalous magnetic moment [42–45]. In particular, the results presented in this article clarify the asymptotic behavior of the γ^*-f_0 form factors.

Acknowledgements Thanks to Volodya Braun and Andreas Schäfer for suggesting this study and for discussions. The work is supported in part by the BMBF, contract number 05P12WRFTE.

Open Access This article is distributed under the terms of the Creative Commons Attribution 4.0 International License (<http://creativecommons.org/licenses/by/4.0/>), which permits unrestricted use, distribution, and reproduction in any medium, provided you give appropriate credit to the original author(s) and the source, provide a link to the Creative Commons license, and indicate if changes were made. Funded by SCOAP³.

References

1. M. Masuda et al. (Belle Collaboration), Phys. Rev. D **93**(3), 032003 (2016)
2. G.A. Schuler, F.A. Berends, R. van Gulik, Nucl. Phys. B **523**, 423 (1998)
3. G.T. Bodwin, E. Braaten, G.P. Lepage, Phys. Rev. D **51**, 1125 (1995)
4. G.T. Bodwin, E. Braaten, G.P. Lepage, Phys. Rev. D **55**, 5853 (1997)
5. V. Pascalutsa, V. Pauk, M. Vanderhaeghen, Phys. Rev. D **85**, 116001 (2012)
6. V.M. Braun, N. Kivel, M. Strohmaier, A.A. Vladimirov, JHEP **1606**, 039 (2016)
7. N.N. Achasov, A.V. Kiselev, G.N. Shestakov, JETP Lett. **102**(9), 571 (2015)
8. N.N. Achasov, A.V. Kiselev, G.N. Shestakov, Pisma. Zh. Eksp. Teor. Fiz. **102**(9), 655 (2015)
9. M. Diehl, T. Gousset, B. Pire, O. Teryaev, Phys. Rev. Lett. **81**, 1782 (1998)
10. K.A. Olive et al. (Particle Data Group Collaboration), Chin. Phys. C **38**, 090001 (2014) [update 2015]
11. W. Ochs, J. Phys. G **40**, 043001 (2013)
12. H.Y. Cheng, C.K. Chua, K.C. Yang, Phys. Rev. D **73**, 014017 (2006)
13. S. Stone, L. Zhang, Phys. Rev. Lett. **111**(6), 062001 (2013)
14. Z.Q. Zhang, S.Y. Wang, X.K. Ma, Phys. Rev. D **93**(5), 054034 (2016)
15. R.L. Jaffe, F. Wilczek, Phys. Rev. Lett. **91**, 232003 (2003)
16. L. Maiani, F. Piccinini, A.D. Polosa, V. Riquer, Phys. Rev. Lett. **93**, 212002 (2004)
17. G. 't Hooft, G. Isidori, L. Maiani, A.D. Polosa, V. Riquer, Phys. Lett. B **662**, 424 (2008)
18. V. Baru, J. Haidenbauer, C. Hanhart, Y. Kalashnikova, A.E. Kudryavtsev, Phys. Lett. B **586**, 53 (2004)
19. G.P. Lepage, S.J. Brodsky, Phys. Lett. B **87**, 359 (1979)
20. S.J. Brodsky, T. Huang, G.P. Lepage, Conf. Proc. C **810816**, 143 (1981)
21. P.A.M. Dirac, Rev. Mod. Phys. **21**, 392 (1949)

22. H. Leutwyler, J. Stern, *Ann. Phys.* **112**, 94 (1978)
23. J. Bolz, P. Kroll, J.G. Körner, *Z. Phys. A* **350**, 145 (1994)
24. Z. Dziembowski, *Phys. Rev. D* **37**, 768 (1988)
25. F. Hussain, J.G. Körner, G. Thompson, *Ann. Phys.* **206**, 334 (1991)
26. X.D. Ji, J.P. Ma, F. Yuan, *Eur. Phys. J. C* **33**, 75 (2004)
27. M. Beneke, G. Buchalla, M. Neubert, C.T. Sachrajda, *Nucl. Phys. B* **591**, 313 (2000)
28. J. Bolz, P. Kroll, G.A. Schuler, *Eur. Phys. J. C* **2**, 705 (1998)
29. V.L. Chernyak, A.R. Zhitnitsky, *Phys. Rep.* **112**, 173 (1984)
30. C.D. Lu, Y.M. Wang, H. Zou, *Phys. Rev. D* **75**, 056001 (2007)
31. M. Beneke, T. Feldmann, *Nucl. Phys. B* **592**, 3 (2001)
32. H.W. Huang, R. Jakob, P. Kroll, K. Passek-Kumericki, *Eur. Phys. J. C* **33**, 91 (2004)
33. P. Kroll, *Eur. Phys. J. C* **71**, 1623 (2011)
34. S.V. Goloskokov, P. Kroll, *Eur. Phys. J. C* **65**, 137 (2010)
35. F. De Fazio, M.R. Pennington, *Phys. Lett. B* **521**, 15 (2001)
36. I. Bediaga, F.S. Navarra, M. Nielsen, *Phys. Lett. B* **579**, 59 (2004)
37. M. Diehl, P. Kroll, C. Vogt, *Eur. Phys. J. C* **22**, 439 (2001)
38. H.N. Li, G.F. Sterman, *Nucl. Phys. B* **381**, 129 (1992)
39. T. Feldmann, P. Kroll, B. Stech, *Phys. Rev. D* **58**, 114006 (1998)
40. P. Kroll, K. Passek-Kumericki, *Phys. Rev. D* **67**, 054017 (2003)
41. H.Y. Cheng, K.C. Yang, *Phys. Rev. D* **71**, 054020 (2005)
42. V. Pauk, M. Vanderhaeghen, *Eur. Phys. J. C* **74**(8), 3008 (2014)
43. G. Colangelo, M. Hoferichter, M. Procura, P. Stoffer, *JHEP* **1409**, 091 (2014)
44. A.E. Dorokhov, A.E. Radzhabov, A.S. Zhevlakov, *Eur. Phys. J. C* **75**(9), 417 (2015)
45. F. Jegerlehner, A. Nyffeler, *Phys. Rep.* **477**, 1 (2009)